

## Stroboscopic microscopy of ferroelectric liquid crystals

Jiuzhi Xue

*Department of Physics, Princeton University, Princeton, New Jersey 08540*

Noel A. Clark

*Department of Physics and Optoelectronic Computing Systems Center, University of Colorado, Boulder, Colorado 80309*

(Received 22 April 1993)

We have studied the switching of surface-stabilized ferroelectric-liquid-crystal (SSFLC) cells using stroboscopic microscopy. We find that the switching process in the chevron-layer-shaped SSFLC's is mediated by domains that occur at the chevron interface and that are nucleated both heterogeneously and homogeneously; that some features of the growth of the domains can be described well by existing theories; and that the peculiar terminal "speedboat" shape of the domains is a function of the applied electric field and the sample temperature. We examine the possible mechanisms that result in asymmetries in domain-wall velocities.

PACS number(s): 83.70.Jr, 61.30.Cz, 77.80.Fm

### I. INTRODUCTION

In recent years, the surface-stabilized ferroelectric-liquid-crystal (SSFLC) structure [1] has attracted much attention due to its potential electro-optic applications. The dynamics of the SSFLC light valve have been treated theoretically assuming the ferroelectric-liquid-crystal (FLC) director  $\mathbf{n}$  rotates collectively on the tilt cone during the switching process [2–4]. Experimentally, Handschy and Clark [5] first directly probed the SSFLC switching process and domains using a stroboscopic microscopy technique. Similar techniques and sample cell structures have been used by Orihara and Ishibashi to study the switching process in SSFLC's, and nucleation and domain growth [6], and by Ouchi, Takezoe, and Fukuda [7], who observed the internal disclination loops during the switching process while growing these switching domains exhibit a striking polygonal shape.

In this paper, we describe an extension of the work of Handschy and Clark using a modified experimental setup. We present experimental results on SSFLC domain-wall velocity and the kinetics of the domain switching and on the dependence of the shape and dynamics of the domain walls on the cell temperature and applied electric field. We discuss the director structures, in particular the structures in the cores of the domain walls, and their symmetries during a switching process. We explicitly calculate the contributions to the domain-wall motion from ferroelectric, dielectric, elastic, viscous, and flexoelectric effects, and examine possible mechanisms that may determine the exotic shape of the reversing domains. We conclude that backflow is the likely cause.

### II. EXPERIMENT AND RESULTS

Unless otherwise noted, this work has been carried out using the Displaytech mixture [8], a ma-

terial similar to that used in earlier x-ray [9] and surface-switching studies [10]. The FLC was sandwiched between two indium tin oxide (ITO) coated glass plates about  $2\ \mu\text{m}$  apart to form the SSFLC geometry. The cell is slowly cooled ( $1\ ^\circ\text{C}/\text{h}$ ) from the isotropic phase to the smectic-*A* (Sm-*A*) phase and further to the smectic-*C\** (Sm-*C\**) phase to obtain large areas with uniform chevron smectic-layer orientations. It has been shown using x-ray scattering that SSFLC's so prepared have the chevron local layer structure [9]. The strobe light used in our experiment is from a homemade dye laser pumped by a XeCl excimer laser with a light pulse duration of 14 ns, which is short enough to "freeze" the sample at a given instant. A single laser pulse is intense enough to give a good illumination of the microscope and sufficiently expose a black and white ASA 400 film.

The complete experimental setup is shown in Fig. 1. The temperature-controlled SSFLC cell is observed under a Nikon Optiphot-Pol transmission polarized light microscope which is illuminated by the pulsed dye laser guided to the microscope through a bundle of optic fibers. The optic fiber bundle converts the point light source of the laser beam into an extended light source, spoiling the spatial coherence and giving nearly Kohler illumination of the microscope. A pulse controller determines the timing sequence of the experiment: it first sends out a pulse to the excimer laser, then after a fixed time interval long enough to charge up the capacitor of the laser, it fires the second pulse to a pulse generator, which in turn sends out first a negative voltage pulse to switch the SSFLC sample cell to its initial state (BRIGHT) then a positive voltage step to switch the cell to the final state (DARK); after a controlled time  $\Delta t$ , the third and the final pulse is sent out to fire the excimer laser which then pumps the dye laser and sends out a visible laser pulse virtually at this instant, enabling the switching process during the second electric voltage pulse, or the process of switching from BRIGHT to DARK, to be observed and

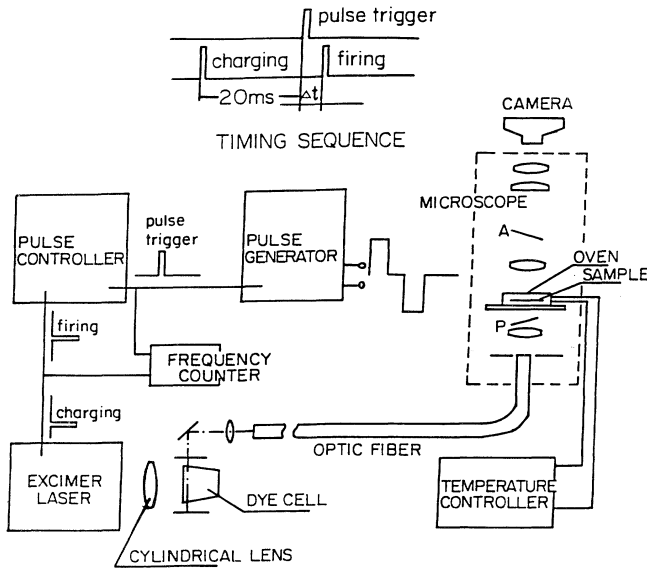


FIG. 1. Experimental setup for the stroboscopic experiment.

photographed.

The basic features observed in the experiment are similar to what Handschy and Clark [5] found, namely a rotation of the effective optic axis of the bulk FLC which can be understood in the frame of the theory of collective director rotation under the applied electric field [11,12] and a switching process mediated by domains which are oval when small [5]. These domains can be nucleated both heterogeneously, as observed by Handschy and Clark [5], and homogeneously, and show a voltage-time threshold behavior dependent on the sample temperature. The homogeneously nucleated domains appear in different places as the switch and illumination process is repeated, and the nucleation mechanism is presumably due to thermal fluctuations. Figures 2 and 3 show some photomicrographs taken for the heterogeneous and homogeneously nucleated domains and their growth as a function of time.

The contrast of the reversing domains decreases quickly as the applied voltage is increased, making it very difficult to photograph as originally designed. However, we found that in the case where domains only partially cover the cell, the sample relaxes back to its initial state,

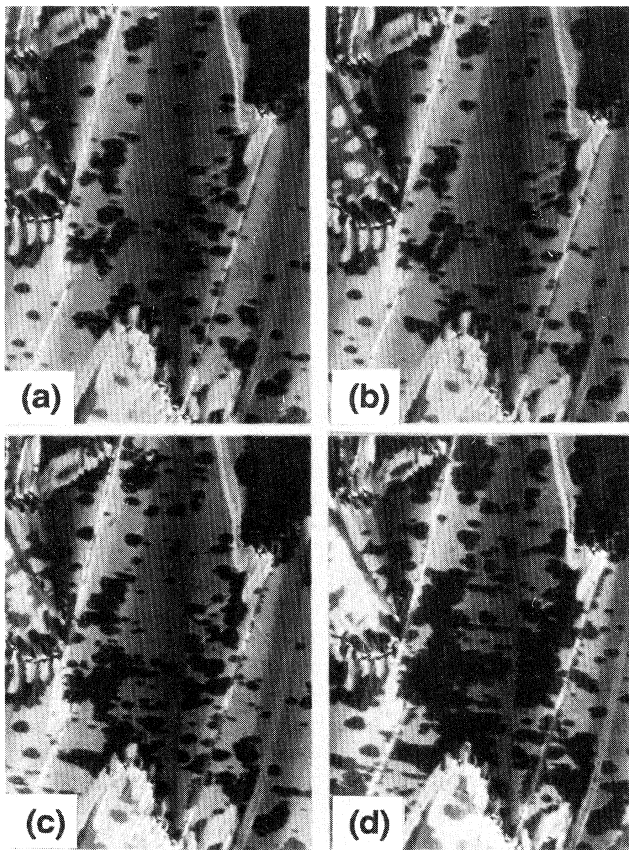


FIG. 2. Heterogeneous nucleation of reversing domains in SSFLC's. The sample temperature  $T = 35^\circ$  and the applied voltage  $V$  is 5 V. Pictures taken after the field is applied to the cell for  $\Delta t$  which is (a) 0.997 ms, (b) 1.368 ms, (c) 1.973 ms, and (d) 3.10 ms. The arrow is  $70 \mu\text{m}$  in length.

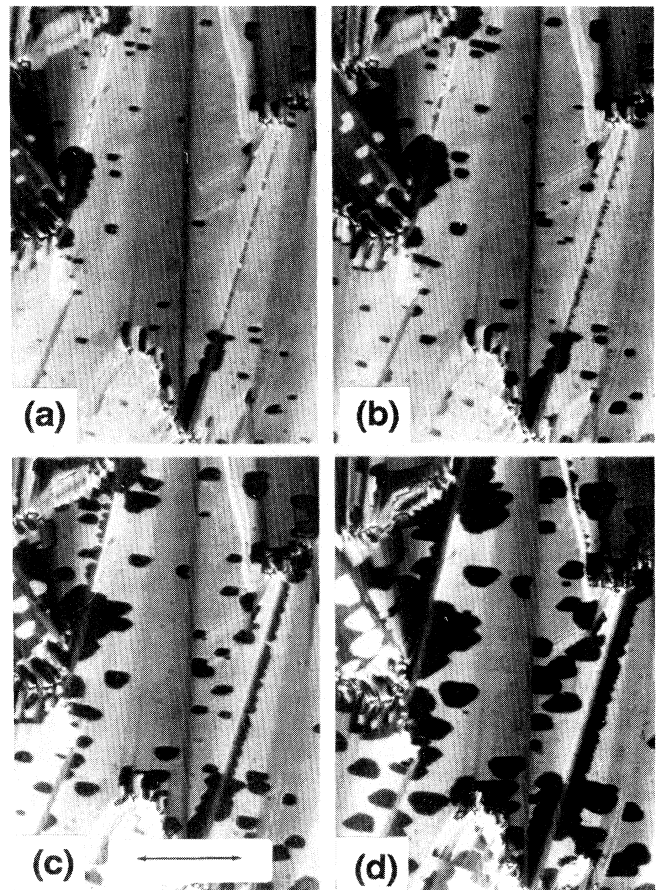


FIG. 3. Homogeneous nucleation of reversing domains in SSFLC's. The sample temperature  $T = 40^\circ\text{C}$  and the applied field  $V$  is 5 V.  $\Delta t$  is (a) 3.48 ms, (b) 3.48 ms [same as for (a)], (c) 3.64 ms, and (d) 3.86 ms.

with a relaxation time for the domains much longer than that for the bulk sample after the removal of the switching electric field, a feature now used to obtain grey level switching in SSFLC's [13,14], and a feature that we use to enhance the contrast of the domains by taking photographs after the bulk relaxed back to its initial state.

### III. DOMAIN GROWTH

Around foreign particles, for example, dust particles or the spacers of the cell, or around defects, the liquid-crystal (LC) director must be nonuniform and deformed. Compared with the areas with director orientation uniform in the cell plane, the director adjacent to these deformed structures is easier to switch when an external reversal field is applied, due to pretilt of polarization caused by the structures. As long as the foreign particles and the defects do not move, new domains will be nucleated from the same places every time when the switching-reversing sequence is repeated. The threshold for these heterogeneously nucleated domains can be fairly low, about  $1 \text{ V}/\mu\text{m}$  for the Displaytech mixture. When there are many foreign particles and a low-amplitude long-duration reversal field is applied, the whole switching process is dictated by the heterogeneous nucleation process, as observed previously [5,6]. When the amplitude of the external field is increased, director fluctuations due to thermal agitation may be large enough to produce a nucleation site for the reversing domains. Due to the stochastic nature of the mechanism, these homogeneous nucleation sites are random in space and time.

The homogeneous nucleation process shows threshold behavior. As the temperature is increased, thermal fluctuations increase and the threshold voltage decreases. The temperature dependence of the threshold behavior for the homogeneous nucleation process is plotted in

Fig. 4 for the Displaytech mixture and a second FLC mixture [15].

The growth of the domains is analyzed by using an advanced image processing system to measure selected areas vs time. For a single heterogeneously nucleated domain, the characteristic length  $l_c$ , defined as the square root of the area measured, is fit to

$$l_c = v(t - t_0), \quad (1)$$

where  $v$  is a characteristic velocity which is essentially the geometric average of the growing rates of the various facets, or the major and minor axes when the domains are approximated as ellipses [5], and  $t_0$  is the time the domain nucleated. Both  $v$  and  $t_0$  are used as fitting parameters here. Figure 5 shows some typical results of the measurements along with the fits for the heterogeneously nucleated domains. As can be readily seen, the domain growth can be described very well using the proposed function form, which indicates that the domain-wall velocity is constant in time, as discussed by Handschy and Clark for domains of dimension large compared to the sample thickness [5].

Figure 6 shows characteristic velocity  $v$  calculated from the above fitting procedure as a function of the applied voltage  $V$  at different temperatures. It is readily seen that  $v$  increases linearly with  $V$  at a given temperature, also as predicted by Handschy and Clark [5]. The solid lines in the figure are best fits to  $v = \alpha(T)V$ , where  $\alpha(T)$  is a constant independent of  $V$ . In Fig. 7 we plot the parameter  $\alpha$  found in the experiment as a function of temperature. A rough estimation by Handschy and Clark [5] shows that  $\alpha$  is inversely proportional to the viscosity and the elastic constant, both of which decrease as the temperature is increased, resulting in an increasing  $\alpha$  as the temperature is increased.

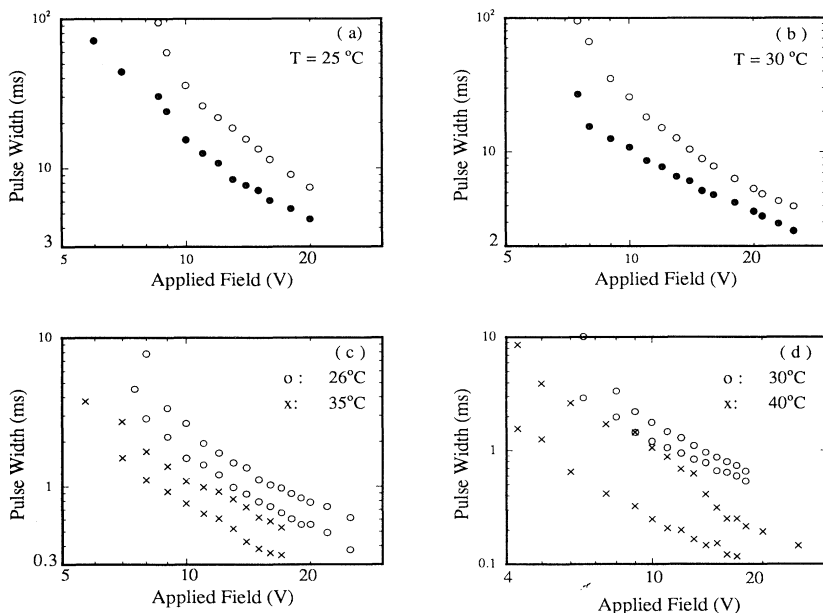


FIG. 4. The threshold behavior for the spontaneous nucleation of switching domains in SSFLC's at the indicated temperatures for (a) and (b) the Displaytech Mixture, and (c) and (d) a second FLC mixture [15]. In each case the lower curve indicates that the homogeneous nucleation process was first observed and the upper curve the switching of the cell completed.

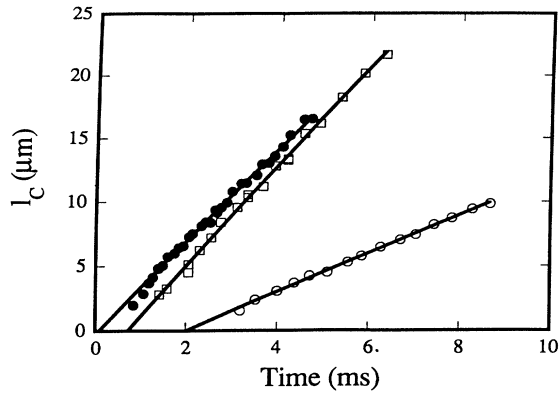


FIG. 5. Characteristic domain length  $l_c$  as a function of time for some well-defined domains.  $\circ$ :  $T = 25^\circ\text{C}$ ,  $V = 3\text{ V}$ .  $\square$ :  $T = 25^\circ\text{C}$ ,  $V = 8\text{ V}$ .  $\diamond$ :  $T = 35^\circ\text{C}$ ,  $V = 3\text{ V}$ . The solid lines are fits to the function  $l_c = v(t - t_0)$ .

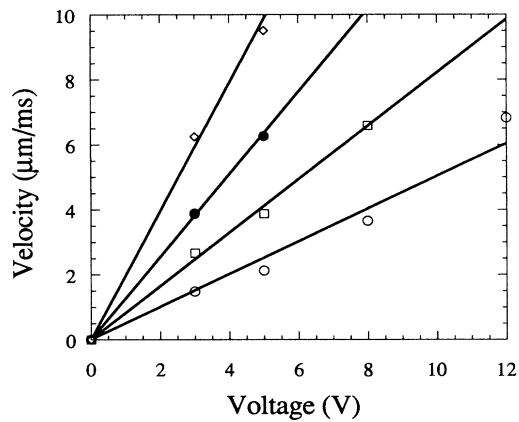


FIG. 6. Characteristic velocity vs applied voltage as a function of temperature  $T$ .  $\circ$ :  $T = 25^\circ\text{C}$ .  $\square$ :  $T = 30^\circ\text{C}$ .  $\bullet$ :  $T = 35^\circ\text{C}$ .  $\diamond$ :  $T = 40^\circ\text{C}$ . The solid lines are the best fits to the function  $v = \alpha V$ .

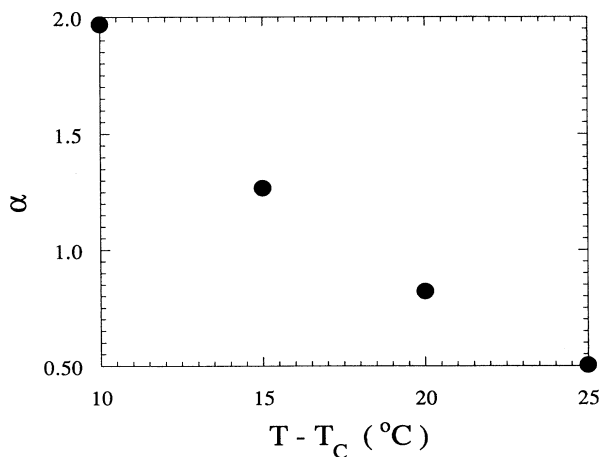


FIG. 7. Temperature dependence of the constant  $\alpha$ .

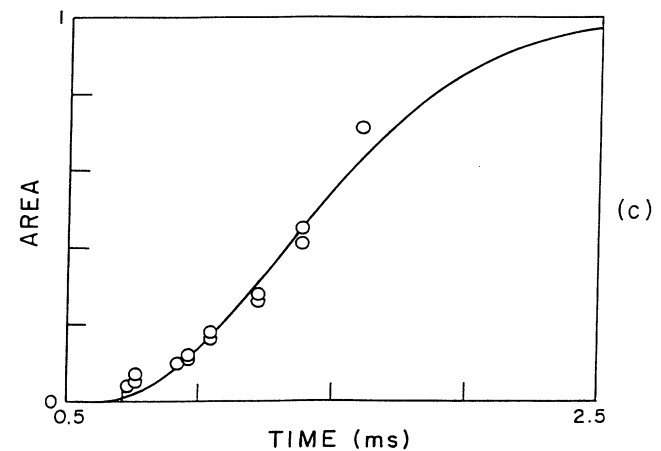
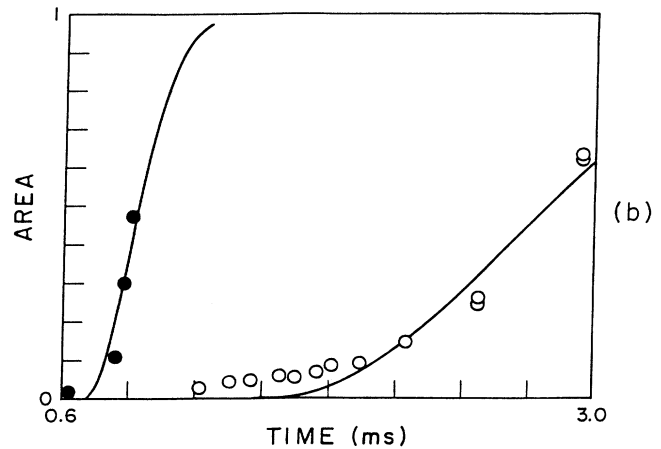
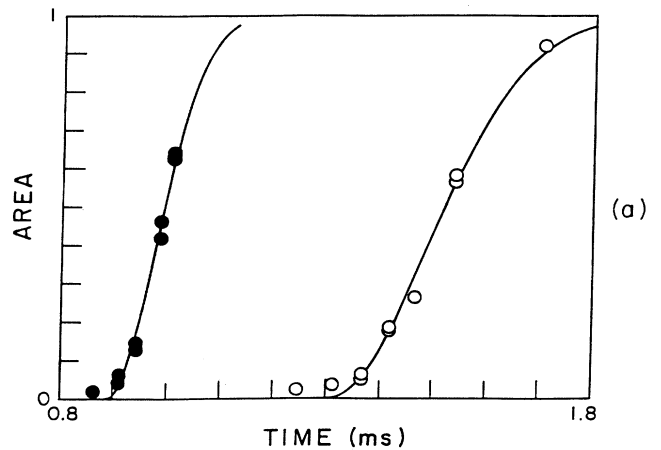


FIG. 8. Fraction of the areas switched in the presence of homogeneous nucleation and domain overlapping at different temperatures and different applied voltages. (a)  $\circ$ : Temperature  $T = 25^\circ\text{C}$ , and the applied field  $V = 12\text{ V}$ ;  $\bullet$ :  $T = 25^\circ\text{C}$ ,  $V = 15\text{ V}$ . (b)  $\circ$ :  $T = 30^\circ\text{C}$ ,  $V = 8\text{ V}$ ;  $\bullet$ :  $T = 30^\circ\text{C}$ ,  $V = 12\text{ V}$ . (c)  $T = 40^\circ\text{C}$ ,  $V = 5\text{ V}$ . The switching processes are dominated by the growth of the homogeneously nucleated domains in all cases except in (b) when  $V = 8\text{ V}$  where the growth of the heterogeneously nucleated domains dominates the switching process. The solid curves are fits to Eq. (2).

When there is homogeneous nucleation and the domains start to overlap, the only appropriate way of characterizing the switching process is to measure the overall fraction of the area switched, as first adopted by Orihara and Ishibashi, who used Avrami's theory of phase change to analyze their heterogeneous nucleation results [6]. Figure 8 shows the measured fraction  $S(t)/S_0$  of area switched as a function of time under certain experimental conditions along with the best fits to the function form developed from the Avrami model [6]

$$S(t)/S_0 = 1 - e^{-a(t-t_0)^2}, \quad (2)$$

where  $a$  is a constant proportional to  $v^2$  and  $t_0$  is a time constant, which essentially indicates when the nucleation of reversing domains starts. From the data we have, we find that the Avrami model describes the switching process well if the dominant nucleation mechanism is the homogeneous nucleation, as illustrated in Fig. 8.

#### IV. THE SPEEDBOAT SHAPE OF THE REVERSING DOMAINS

It is noticeable from Figs. 2 and 3 that, although their starting shape is round or oval, the reversing domains quickly grow into rather peculiar shapes, often irregular pentagons or "speedboats," as first observed and named by Ouchi, Takezoe, and Fukuda [7], indicating different domain-wall velocities in different directions. The facets suggest cusplike minima in  $v(\beta)$ , where  $\beta$  is the local propagation direction of the wall, in analogy with minima in surface energies which produce crystal faceting [16].

At low temperature (25 °C), the reversing domains gradually grow into irregular trapezoids at applied voltages of 3 V and 5 V (cf. Fig. 9) with domain-wall velocities which are very asymmetric both along the  $z$  axes, the projection of the smectic layer normal on the surface, as indicated by the direction of the zigzag walls [17,18], and in the smectic-layer  $y$  direction (see Fig. 12 for coordinates). We define that the  $+z$  axis is pointing in the chevron direction, i.e., the smectic layers buckle towards  $+z$  axis in the middle of the sample. We then find that the domain wall in the  $-z$  direction always moves at a much slower speed compared to that moving in the  $+z$  direction, although both are local minima, regardless of the sign of the applied switching voltage. As we go across a zigzag wall, the chevron buckling changes direction and the asymmetry in the domain-wall velocity also reverses, resulting in a "flip" of the reversing domains (mirror image of the domains about the  $xy$  plane). This flip is understandable in view of the coupling of the polarization pretilt and larger tilt at the chevron interface [18-21]. The domain walls moving in the smectic-layer direction show similar asymmetry in speed, i.e., the walls moving along the  $-y$  direction have very different speed than those moving along the  $+y$  direction. However, this asymmetry of the domain-wall velocity in the smectic layer differs from that in the  $z$  axis in that the asymmetry reverses not only when going across the zigzag walls but also when the switching process is reversed. That is, the walls in the  $+y$  direction will move

slower when across a zigzag wall and when the applied voltage changes sign, if they were moving faster before. This direction dependence of the domain-wall velocity results in the peculiar shape of the reversing domains: assuming that in the smectic layer the walls move slower in the  $-y$  direction, combined with the slow speed in the  $-z$  direction, we observe the flat stern of the speedboats, the two local minima velocities along  $+z$  and  $-z$  directions giving rise to the frame of the "boats," and the combination of a faster speed in the  $+y$  direction and the asymmetry in the  $z$  directions resulting in the asymmetric pointed "bow" of the speedboats. The orientation of these features relative to the cell geometry is discussed in Sec. V. As the switching process is reversed, the asymmetry in the domain-wall velocity in the smectic layer is reversed, resulting in the speedboats pointing in opposite directions. At low voltage, the stern velocity can be much smaller ( $< 0.05$ ) than that of the other side. This faceting is a feature of a steady-state dynamic process, i.e., well defined only when the domains are growing. At very low or zero voltage they lose their shape as the force due to pinning on defects become large compared to those

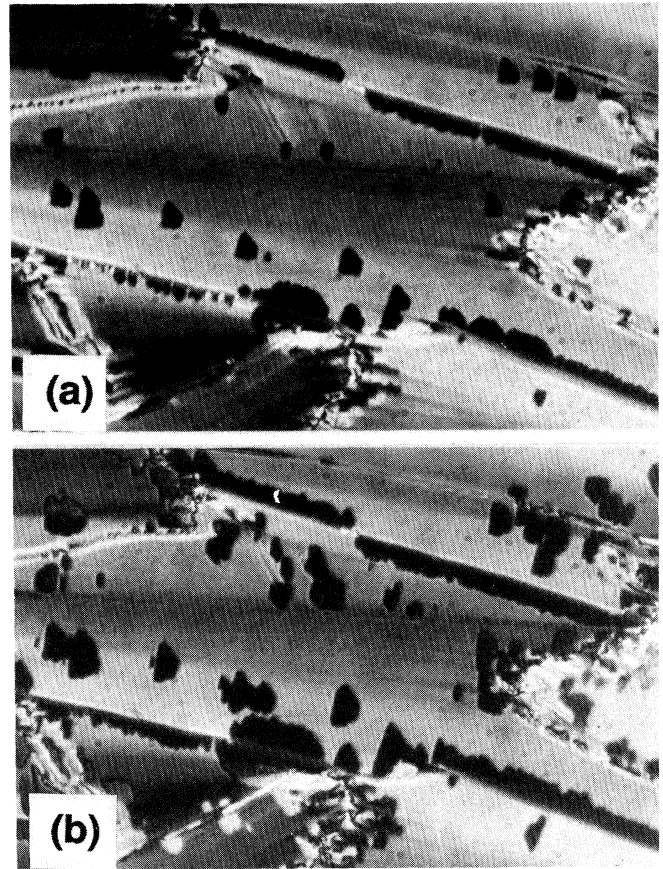


FIG. 9. Photomicrographs of the reversing domains when  $T = 25^\circ\text{C}$ . The pictures were taken when the (a) 5 V voltage is applied for 5.582 ms and (b) 8 V applied for 4.243 ms. Notice that the asymmetry of the domains is becoming less pronounced in (b).

determining the motion.

As the applied voltage is increased to 8 V, the asymmetry of the domain-wall velocity along  $y$  becomes less pronounced [as shown in Fig. 9(b)]; however, the increase in the voltage seems to have quite small effects on the asymmetry of domain-wall velocities along  $z$ , resulting in the sterns becoming more like the bows and the domains becoming very asymmetric hexagons. When the voltage is increased to 12 V and 15 V, the growth of the homogeneously nucleated domains dominates, the domain-wall velocities in the  $+y$  and  $-y$  directions become nearly the same, as seen in the photomicrographs taken at 12 V and 15 V in Fig. 10.

As the temperature is increased, the difference between domain-wall velocities in both the smectic layer and the  $z$  directions becomes smaller and smaller, and the domains become more and more like symmetric hexagons, as shown in Fig. 11.

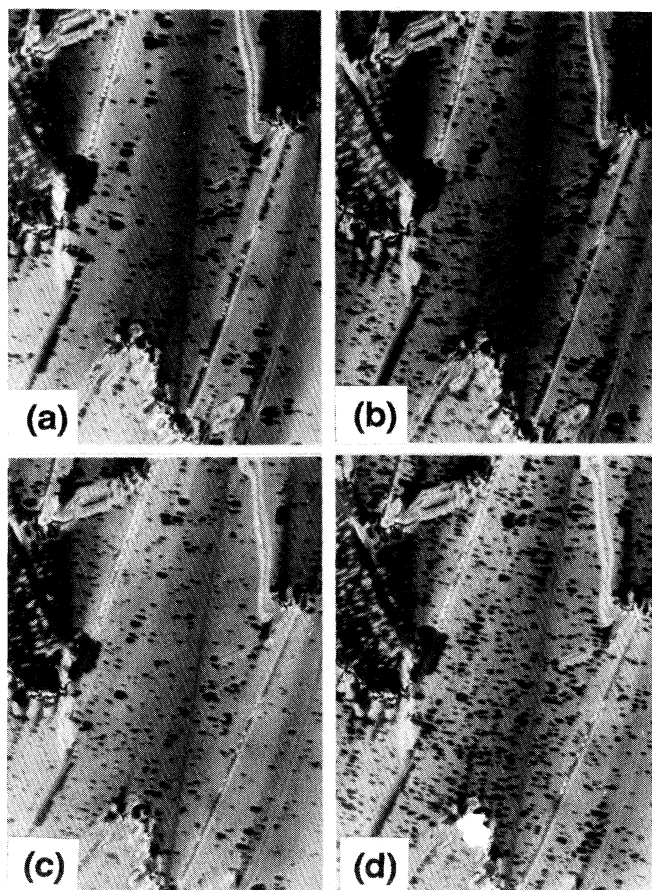


FIG. 10. Photomicrographs of the reversing domains when  $T = 25^\circ\text{C}$  and the applied field is higher.  $V = 12$  V in (a) and (b) with  $\Delta t$  being 1.368 ms and 1.418 ms, respectively. The applied field is 15 V in (c) and (d) with the  $\Delta t$  being 0.911 ms and 0.942 ms, respectively. Notice that the domains are getting more symmetric and homogeneous nucleation dominates the switching process.

## V. THE SWITCHING PROCESS IN CHEVRON-LAYER SSFLC'S

Handschy and Clark in the original study of the transient reversing domains attributed them to a first-order director-polarization  $\mathbf{n}$ - $\mathbf{P}$  reorientation transition between surface stabilized states with director reorientation at the FLC-ITO interface during the switching process. Such a mechanism, however, should give rise to two sets of domains focused at slightly different positions due to the two independent glass-FLC interfaces. However, only one set of the domains was observed both in their experiments and the current experiments. Ouchi, Takezoe, and Fukuda first observed that the director in the top and bottom halves of the cell rotates differently as a result of opposite polarization pretilt on the two FLC-solid interfaces and an internal disclination loop is formed interior to the cell. They proposed a switching mechanism

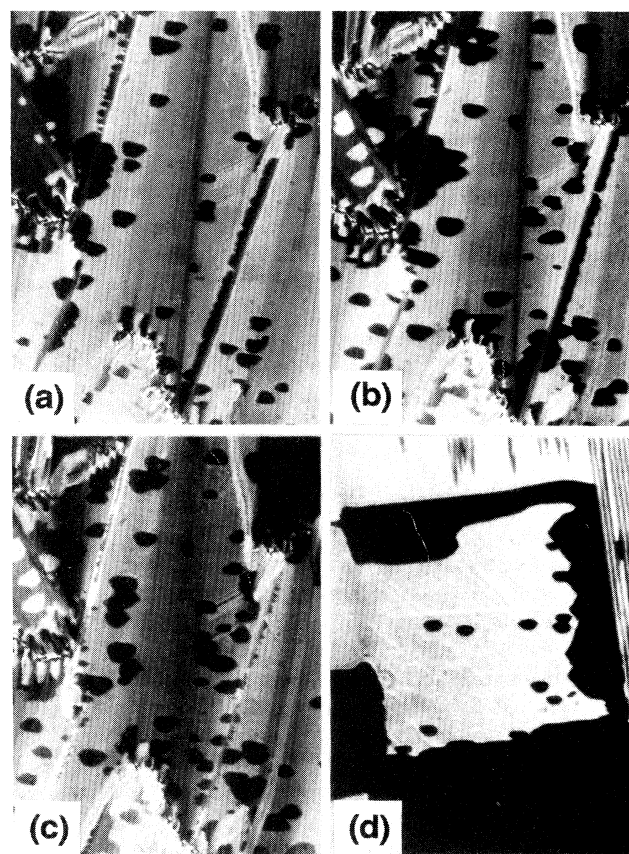


FIG. 11. Photomicrographs of the reversing domains at higher temperatures. (a)  $T = 30^\circ\text{C}$ , applied field  $V = 5$  V, and the time  $\Delta t = 3.30$  ms. (b)  $T = 35^\circ\text{C}$ ,  $V = 5$  V,  $\Delta t = 2.183$  ms. (c)  $T = 40^\circ\text{C}$ ,  $V = 3$  V,  $\Delta t = 2.764$  ms. (d). The sample is shear aligned and the material is the second FLC mix.  $T = 40^\circ\text{C}$ ,  $V = 1$  V, and  $\Delta t = 1.49$  ms. Notice that the domains getting more and more symmetric about the chevron direction.

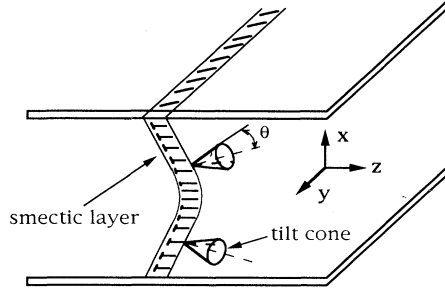


FIG. 12. The director structure during the chevron interface switching. The smectic layer is assumed to have a smooth change near the interface. The elasticity forces the molecular tilt angle at the chevron interface to go to zero during the switching process, which causes energy and makes the chevron interface act like another surface.

assuming that the smectic layers are still perpendicular to the substrates [7].

It was then shown that the smectic layers assume a chevron structure in planar-treated cells [9,11,17] leading to a proposal that the director field is orientationally stabilized as the chevron interfaces divide the cell

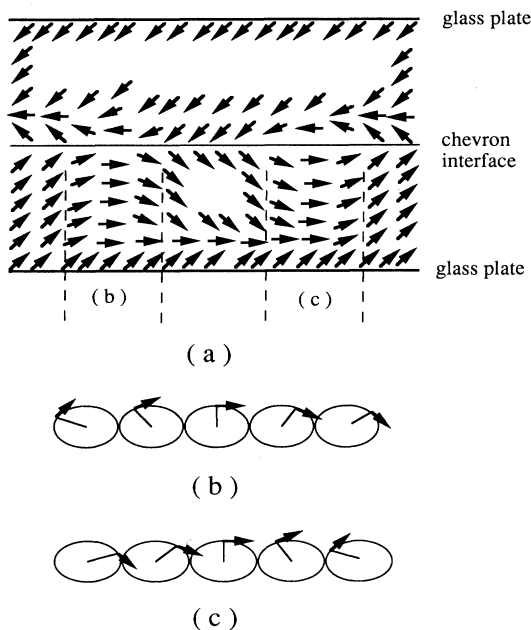


FIG. 13. Polarization structure of a partially switched chevron cell. The surface favors  $\mathbf{P}$  pointing into the FLC. The cell is initially in  $\mathbf{P}$  up state. When a field pointing down is applied,  $\mathbf{P}$  is forced to reorient to minimize the energy. In the picture, the middle part of the cell including the chevron interface is switched to down state, and the  $\mathbf{P}$  structure in this area is uniformly down in the top half of the cell and splayed in the bottom half of the cell. In the area where chevron interface is still not switched, the  $\mathbf{P}$  structure is still splayed in the top half of the cell and close to be uniformly up in the bottom half of the cell. The chevron points toward the reader. Notice the domain wall boundary is mainly a  $\pi$  wall. (b) and (c) c director structure across the indicated  $\pi$  walls in (a).

into two parts along  $x$  to produce the so-called “half-splayed” states. An applied field initially reorients director  $\mathbf{n}$  at places away from the interface, leaving a thin layer near the chevron interface which switches via surface domains at a later time to produce the domains observed, as shown in Figs. 12 and 13 [11,17].

An independent experiment revealed that the director field near the FLC-solid interface does not switch in chevron cells when the applied field is small [10]. On the other hand, the existence of the chevron interface, its switching as a domain-mediated process agrees well with a variety of experimental observations [12,19,22,23]. The chevron interface can be described in a way similar to the other two (FLC-solid interface) surfaces with an interaction energy  $g_i = \gamma \cos \Psi$ , where  $\Psi$  is the angular jump in the director orientation as the chevron interface is crossed [11,17]. With typical elastic constants [11],  $\gamma = 0.7 \text{ erg/cm}^2$  [24], which is similar to the interaction strength between FLC and the glass surface [10].

We now consider a chevron cell with the chevron interface at middle of the cell shown in Fig. 12. Assuming that the solid-FLC interaction favors  $\mathbf{P}$  pointing towards the FLC [10] and that initially  $\mathbf{P}$  is splayed in the top half and uniformly pointing up in the bottom half (half-splayed up state), after a down electric field  $E$  is applied, LC molecules in the top half should respond to the external field on the time scale of  $\tau_0 = \eta/PE$ , where  $\eta$  is the rotational viscous coefficient, except in a thin layer near the chevron interface where the elastic force from the chevron interface interaction plays an important role. The  $\mathbf{P}$  structure in the top half is thus uniformly pointing down in regions where the interface is switched and splayed where the interface is not switched. In the bottom half, if the chevron interface is switched,  $\mathbf{P}$  is splayed in a thin layer near the FLC-solid and uniformly pointing down elsewhere. In regions where the chevron interface is not switched,  $\mathbf{P}$  structure depends on the strength of the applied electric field. If the field correlation length  $\xi_e = \sqrt{\frac{K}{PE}}$  is less than  $l/4$ , where  $l$  is the cell thickness, the  $\mathbf{P}$  structure tends to be uniformly pointing down near the middle of the half (cf. Fig. 13), the domain switching in this case involves a thin layer of molecules near the chevron interface and the domain boundary is a surface domain wall on the chevron interface [11,17]. If the applied voltage is low such that  $\xi_e > l/4$ , the  $\mathbf{P}$  structure is distorted throughout the cell, as illustrated in Fig. 13. This implies that the chevron interface switching at lower applied field involves bulk switching as well as surface domain motion.

## VI. THEORETICAL CONSIDERATIONS OF THE DOMAIN WALLS

The experimental observations show that the domain-wall velocity is direction dependent, especially at lower applied fields and at lower temperatures, which results in the peculiar shapes of the reversing domains. In principle, the dynamics of the domain walls depends on the electric and elasto-hydrodynamic properties of the FLC. However, the detailed equation of motion for domain

walls is very complicated and is determined by the balance between ferroelectric, elastic, dielectric, and flexoelectric torques. It is also highly possible that the hydrodynamic interactions, which produce viscous torques and backflow [25], are important in the system. In what follows, we consider a simplified sample geometry in an effort to understand the sources for the asymmetric domain shape. We take the smectic layers to be tilted with respect to the  $xy$  plane by an angle  $\delta$ . We discuss the director structure of the domain walls traveling in the smectic-layer direction  $y$  and in the  $z$  axis and study their dynamics when the applied electric field is along the  $x$  axis which is perpendicular to the substrate, as shown in Figs. 14 and 16.

### A. Domain walls in the smectic layer direction

As discussed above, when the applied field is small and temperature is low, the domain boundaries are primarily  $\pi$  walls. Here we consider a one-dimensional problem where the azimuthal angle  $\phi$  is allowed to change only in the  $y$  direction (parallel to the smectic layers). Assume  $\mathbf{P}$  is initially pointing up ( $\phi = 0$ ) everywhere. Under application of a reversal field, a region centered around  $y = 0$  is first switched to the  $\mathbf{P}$  down ( $\phi = \pi$ ) state, and the region keeps growing by means of domain-wall motion. As shown in Fig. 14, one of the two domain walls is then traveling along the  $-y$  direction with  $\phi(y)$  changing from 0 to  $\pi$  ( $b$  wall) and the other one is traveling along the  $+y$  direction with  $\phi(y)$  changing from  $\pi$  to 0 ( $c$  wall).

The first thing to notice is that there is a structural asymmetry inherent to the two walls, as shown in Figs. 13(b) and 13(c), related to the sign of the surface domains comprising the domain wall [17,20,21]. Although the  $\mathbf{c}$  director of both walls assumes splayed structures, it has a positive divergence and appears to be unwinding as the wall moves for the ( $b$ ) wall, while for the ( $c$ ) wall, the divergence is negative and the structure tightens as the wall approaches. Careful symmetry considerations allow the examination of the director structure under different experimental conditions: a rotation about the  $x$  axis by  $180^\circ$  reverses the chevron direction, which is equivalent to going across a zigzag wall, and in the laboratory frame changes the position of the two walls; rotating the sample about the  $z$  axis by  $180^\circ$  around the chevron interface is equivalent to reversing the direction of applied electric field, and we again see that the position of the two walls switch. This shows that the asymmetry of the director structures of the two walls is exactly the same as the asymmetry of domain-wall velocities observed experimentally. It is therefore concluded that this director structural difference for the two walls may play a significant role in determining the asymmetry in the domain-

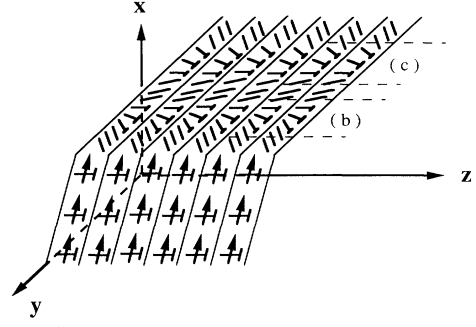


FIG. 14. The simplified model of switching process in the smectic layer direction. The smectic layers are tilted with respect to the  $xy$  plane by an angle  $\delta$ . The azimuthal angle of the director  $\phi = 0$  (corresponding to  $\mathbf{P}$  pointing up) everywhere except in a region around middle where the directors reoriented to  $\phi = \pi$  ( $\mathbf{P}$  down). The two domain walls are different in the sense that ( $b$ ) wall has  $\phi = 0$  changed to  $\phi = \pi$  and the ( $c$ ) wall just the opposite.

wall velocities, particularly as it produces asymmetry in backflow, as discussed below.

The resulting electrical property from a director structure distortion is the appearance of a nonzero flexoelectric polarization  $\mathbf{P}_f$ . Theoretical considerations of flexoelectricity in ferroelectric liquid crystal was first made by Dahl and Lagerwall [26], and by Pikin and Indenbom [27]. Following Dahl and Lagerwall's notation, we get the flexoelectric dipole  $\mathbf{P}_f$  for such a one-dimensional distortion as

$$\begin{aligned} \mathbf{P}_f = & -e_{13} \sin \phi \frac{d\phi}{dx} \mathbf{c} + e_{16} \cos \phi \frac{d\phi}{dx} \mathbf{k} \times \mathbf{c} \\ & + e_{19} \sin \phi \frac{d\phi}{dx} \mathbf{k}, \end{aligned} \quad (3)$$

where  $e_{13}, e_{19}$  are flexoelectric coefficients describing the effect due to the  $\mathbf{c}$  director splay and  $e_{16}$  is the coefficient describing the effect due to the  $\mathbf{c}$  director bend. As readily seen in the above equation, due to the opposite sign for  $\frac{d\phi}{dx}$ , we see that the flexoelectric polarization points in opposite directions for the two walls. This can be most easily demonstrated by the splay of the  $\mathbf{c}$  director, as shown in Figs. 13(b) and 13(c).

The detailed equation of motion for directors in the domain-wall region requires a complete consideration of contributions from electrical, elastic, and hydrodynamic effects. Assuming that there is no smectic-layer distortion with the field [28] and the one-constant approximation in calculating the elastic free energy, the total free energy density due to the distortion  $\phi(y)$ , is given as [24,26]

$$\begin{aligned} F = & \frac{1}{2} B \left( \frac{d\phi}{dx} \right)^2 + D \cos \phi \frac{d\phi}{dx} + PE \cos \delta \cos \phi - \frac{1}{8\pi} \Delta \epsilon E^2 \cos^2 \delta (\sin \phi - \sin \phi_0^2) \\ & + (e_{13} \sin^2 \phi - e_{16} \cos^2 \phi) E \cos \delta \frac{d\phi}{dx} + e_{19} E \sin \phi \sin \delta \frac{d\phi}{dx} - \frac{1}{8\pi} \left( P \sin \phi - (e_{13} + e_{16}) \sin \phi \cos \phi \frac{d\phi}{dx} \right)^2, \end{aligned} \quad (4)$$



where  $\phi_0$  is the azimuthal angle when the director is in the  $yz$  plane,  $B$  and  $D$  are elastic constants,  $\Delta\epsilon$  is the dielectric anisotropy, and the last term is due to the interaction between dipoles. By assuming that the external field  $E$  is a constant, neglecting effects due to backflow but adding in the conventional viscous torque, we get the equation of motion as

$$\begin{aligned} \eta \frac{d\phi}{dt} = & B \frac{d^2\phi}{dx^2} + PE \cos \delta \sin \phi \\ & + \frac{\Delta\epsilon}{4\pi} E^2 \cos^2 \delta (\sin \phi - \sin \phi_0) \cos \phi \\ & + \frac{P^2}{4\pi} \sin \phi \cos \phi \end{aligned} \quad (5)$$

where, by assuming  $e_{ij}$  to be small, we have ignored the higher-order terms due to flexoelectricity in the equation of motion. It is important to note that, unless there is a gradient in the external field in the direction of director distortion, the flexoelectricity does not contribute to the director dynamics in the bulk, and the inclusion of the ferroelectric, dielectric, and flexoelectric torques apparently does not yield any asymmetry for the two walls moving in the opposite directions along the  $y$  axis.

This forces us to consider other effects and assumptions that we made in constructing the equation of motion. It has been recently shown that backflow due to the coupling of molecular orientation and flow could be of significant importance in determining the dynamics of the director [25]. Considering the switching geometry illustrated in Fig. 12, in the absence of a nucleated domain the molecular reorientation accompanying the application of a field will set a flow velocity field  $\mathbf{v}(\mathbf{r}, t) = v_y(x, t)\hat{\mathbf{y}}$ , with  $v_z = 0$  because of the layering and  $v_x = 0$  because we assume the liquid to be incompressible and  $v_x$  to be zero at the solid boundaries. In general the flow is asymmetric with respect to  $\mathbf{y}$ , i.e.,  $\int dx v_y(x) \neq 0$  and there is a net flow in the  $\mathbf{y}$  direction. The flow field possesses the basic lack of symmetry of the speedboat domains in  $\mathbf{y}$ , i.e., one of the walls will travel with the net flow and the other against it. The flow field will depend on distance from the domain walls, i.e., depend on  $\mathbf{x}$  and  $\mathbf{z}$  also. Figure 15(a) shows a sectional view of the speedboat domain in Fig. 13 along with the molecular rotation (open arrows) accompanying domain growth [Fig. 15(b)] and the expected flow pattern [Fig. 15(c)]. As can be seen the  $\ominus$  surface domain wall moves in a direction *opposite* to the flow it generates, whereas the  $\oplus$  surface domain wall moves *along* the flow. We would thus expect the  $\oplus$  velocity to be larger, i.e., the  $\oplus$  line to be the speedboat bow, and the  $\ominus$  line to be the low velocity stern. This is in agreement with the observations of Ouchi and co-workers [20,21], who interpreted the domains as disclination lines in the cell, and with ours in the current experiments. This assignment (stern =  $\ominus$  surface domain and bow =  $\oplus$  surface domain) is independent of switching direction (up to down or down to up) and of the sign of  $\mathbf{P}$ .

The velocities generated by backflow in SSFLC cells have been modeled in the simulation of the coupled elastic hydrodynamic equations, assuming a flow velocity

$\mathbf{V}(\mathbf{r}) = V_y(x)\hat{\mathbf{y}}$  [25]. Since in the present case  $\mathbf{V}$  has both  $x$  and  $y$  components which depend on both  $x$  and  $z$ , the results of these simulations are most directly applicable. However, the flow velocities generated are comparable to the domain-wall velocities found here under similar parameter conditions. Thus backflow appears to affect the wall velocity in the correct qualitative way. There remains to be explained the spectacular faceting, which for the stern may arise as follows: The velocity fields generated above and below the chevron interface are vortex

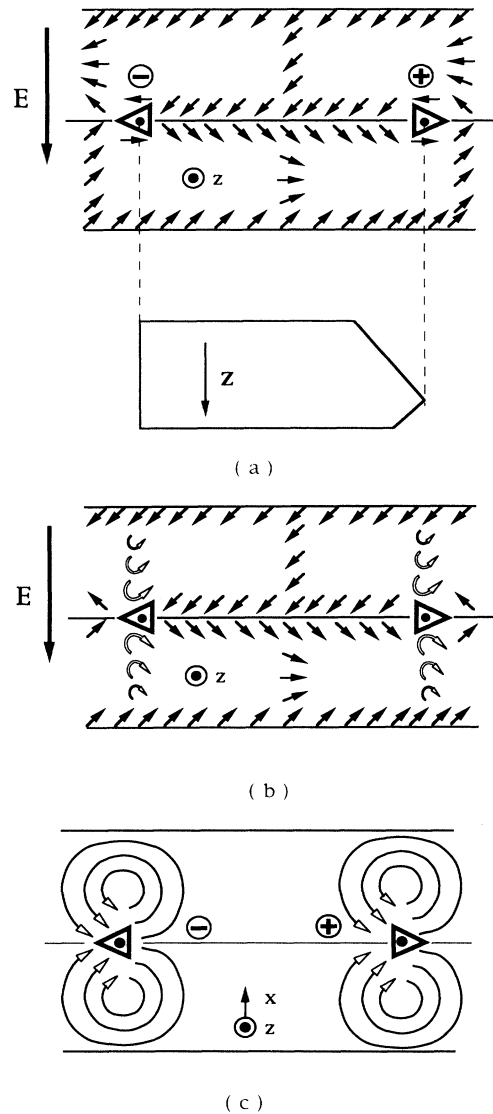


FIG. 15. (a) Sectional view of the polarization distribution in a layer with a speedboat domain expanding in response to a down field showing the surface domains, their disclination strength  $\ominus$ ,  $\oplus$  and their direction of motion ( $\Delta$ ,  $\nabla$ ). (b) Schematic picture of the molecular rotation (open arrows) accompanying wall motion;  $d\phi/dt$  decreases with increasing distance from the wall core. (c) Schematic picture of the resulting flow velocity, showing that the velocity field assists the motion of the  $\oplus$  line, while impeding that of the  $\ominus$  line.

tubes. In the case of the stern the tube runs parallel to the  $z$  axis, i.e., with a  $V_y(x, y)$  that is independent of  $z$ . All gradients of  $V_y$  are in the  $x, y$  plane. However, for the motion of a linear wall oriented at some angle relative to  $z$ , the vortex tube will also be so oriented and we find that the flow velocity  $\mathbf{V}$ , which because of the smectic layering will still be in the  $x, y$  plane, will necessarily develop gradients along  $z$  and in excess dissipation. We thus predict that the flow velocity and its retardation effect will be largest for the observed stern orientation. Quantitative analysis of this behavior is currently being carried out.

Although the flexoelectricity does not contribute to the bulk director dynamics if the electric field is constant,

it influences the director structure and hence the stored energy of the structure via boundary conditions [29]. In the above considerations, we assumed that the domain walls already exist and are infinitely long, which is clearly an idealized model. In a real sample cell, the domain walls are finite in size and length. The defect structure of the walls therefore influences the dynamics in two ways: they alter the local electric field via nonzero electrical dipoles and they store energy as the walls get longer. Here we concentrate on the energy stored by the walls and consider the idea of line tension  $\Gamma_s$ , defined as the total free energy for the wall per unit length in the  $z$  direction. By integrating Eq. (4) with respect to  $y$ , we get

$$\Gamma_s = \int B \frac{d\phi}{dy} d\phi + \int \left( PE \cos \delta \cos \phi - \frac{1}{8\pi} \Delta \epsilon E^2 \cos^2 \delta (\sin \phi - \sin \phi_0)^2 \right) \left( \frac{d\phi}{dy} \right)^{-1} d\phi - \int \frac{P^2}{8\pi} E \cos \delta \left( \frac{d\phi}{dy} \right)^{-1} d\phi + (e_{13} - e_{16}) \frac{\pi}{2} E \cos \delta + 2e_{19} E \sin \delta. \quad (6)$$

Note that the line tension contains contributions from flexoelectricity which depends on the direction of the walls [24]. When the domain grows, its periphery also increases, which increases stored energy. If the line tension depends on the orientation of the domain wall, anisotropic domains may be expected, although the extreme faceting observed would not be expected.

When the applied voltage is increased, the domain walls gradually become the disclination loops as proposed by Handschy and Clark, the domain wall velocities along the  $+y$  and  $-y$  directions became similar, yielding quite symmetric domains, apparently a result of less bulk switching and therefore a smaller influence of the bulk director structure and its resulting flexoelectric and backflow effects.

### B. Domain walls in the chevron direction

The chevron layer structure poses a natural asymmetry in the direction of projection of smectic layer normal to the substrate, the  $z$  axis. Here we consider the switching properties of two domain walls traveling in opposite directions along the  $z$  axis. As illustrated in Fig. 16, we again consider a one-dimensional problem with  $\phi$  changing only in the  $z$  direction. We assume that  $\mathbf{P}$  is originally up ( $\phi = 0$ ) and a region centered around  $z = 0$  is switched to  $\mathbf{P}$  down ( $\phi = \pi$ ) under application of an electric field. As shown in Fig. 16, the two domain walls in this case are then the one traveling along the  $-z$  direction with  $\phi(z)$  changing from 0 to  $\pi$  ( $b$  wall) and the other one traveling along the  $+z$  direction with  $\phi(z)$  changing from  $\pi$  to 0 ( $c$  wall).

Here we also start by examining the director structure and the director kinetics for the two domain walls. As shown in Fig. 16, we find that there is again an asymmetry inherent to the two walls traveling in the  $-z$  ( $b$

wall) and  $+z$  ( $c$  wall) directions. The  $\mathbf{c}$  director for both walls mainly assume a twist structure; however, they twist clockwise for the  $b$  wall and counterclockwise for the  $c$  wall, and during the switching process, the  $b$  wall unwinds and the  $c$  wall tightens, in a way similar to that for domain walls traveling in smectic layers. It is also

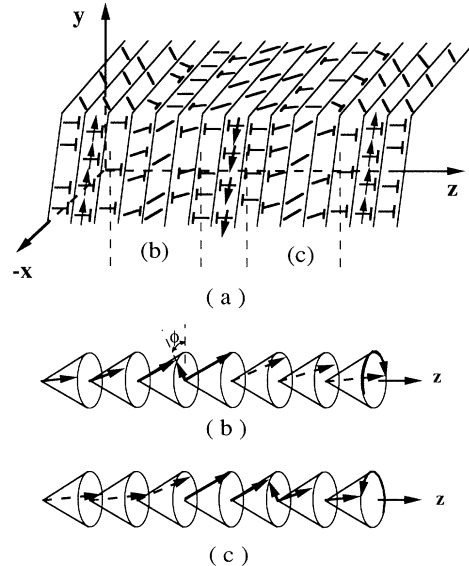


FIG. 16. (a) Simplified model of director reorientation process in the chevron direction. The smectic layers are tilted with respect to the  $xy$  plane by an angle  $\delta$ . The azimuthal angle of the director  $\phi = 0$  (corresponding to  $\mathbf{P}$  pointing up) everywhere except in a region around  $z = 0$  where the directors reoriented to  $\phi = \pi$  ( $\mathbf{P}$  down). The two domain walls are different in the sense that (b) wall has  $\phi = 0$  changed to  $\phi = \pi$  and the (c) just the opposite. (b) and (c): The  $\mathbf{c}$  director structures across the indicated domain walls in (a).

important to note that, although completely suppressed in SSFLC structures, FLC's assume helical structure intrinsically, and one of the domain walls, for example, the  $b$  wall, may be twisting the same way as the intrinsic helix while the other one is against it, depending on the material properties. We thus postulate that this asymmetry in director structure and kinetics is responsible for the asymmetry in domain-wall velocities observed experimentally. Symmetry considerations again show that the asymmetry in the director structure is in agreement with the experimental observations: rotating the sample about the  $y$  axis by  $180^\circ$ , we get the sample with the chevron pointing in the opposite direction, which indicates that across the zigzag walls the asymmetry of the domain-wall velocities are reversed; rotating the sample about the  $z$  axis by  $180^\circ$  is equivalent to reversing the sign of the applied field, an operation that does not change the chevron direction and hence the asymmetry of the domain-wall velocities.

For the detailed dynamics of the domain-wall motion along the  $z$  direction, we can again write down the free energy with contributions from elasticity (including intrinsic helicity in this case), ferroelectricity, dielectricity, flexoelectricity, and viscosity. Treatment similar to that above for the walls in the  $y$  direction shows that, when a constant external electric field is applied, there is no apparent asymmetry in the equations governing the dynamics for walls moving in the  $+z$  and  $-z$  directions due to these contributions. This again suggests that we need to include the effects due to backflow and consider the contribution from line tensions. Overall, the

domain-wall switching should be at least considered as a two-dimensional problem and numerical methods must be exploited to give a detailed description of the dynamical properties of the domains.

In conclusion, we find that the director reorientation process in the chevron-layer-shaped SSFLC's is mediated by reversing domains which are nucleated heterogeneously at lower applied electric fields and both heterogeneously and homogeneously at higher applied voltages and higher temperatures; the domain growth can be described well by the existing theories. Based on experimental observations, we considered the switching mechanisms for SSFLC cells and the director structures during the switching process. We also examined possible mechanisms, in particular the effect of flexoelectricity and backflow, in determining the terminal shape of the domains which depends on the amplitude of the applied voltage and the sample temperature. We concluded that the backflow is the likely cause of the fascinating faceting of the domains observed experimentally.

#### ACKNOWLEDGMENTS

We would like to thank M. A. Handschy, J. E. Maclennan, Z. Zhuang, and Z. Zou for helpful discussions. This work was completed at the University of Colorado and was supported by NSF Engineering Research Center Grant No. CDR 86-22236, ARO Grant No. DAA 03-90-6-0002, and NSF Solid State Chemistry Grant No. DMR 8901657.

- 
- [1] N.A. Clark and S.T. Lagerwall, *Appl. Phys. Lett.* **36**, 899 (1980).
  - [2] J.-Z. Xue, M.A. Handschy, and N.A. Clark, *Ferroelectrics* **73**, 305 (1987).
  - [3] P. Schiller, G. Pelzl, and D. Demus, *Liquid Cryst.* **2**, 21 (1987).
  - [4] M.A. Handschy and N.A. Clark, *Ferroelectrics* **59**, 69 (1984).
  - [5] M.A. Handschy and N.A. Clark, *Appl. Phys. Lett.* **41**, 39 (1982).
  - [6] H. Orihara and Y. Ishibashi, *Jpn. J. Appl. Phys.* **23**, 1274 (1984), and references therein.
  - [7] Y. Ouchi, H. Takezoe, and A. Fukuda, *Jpn. J. Appl. Phys.* **26**, 1 (1984).
  - [8] The FLC mixture is an equal mixture of W7 and W82, which are 4'-[(*s*)-2-ethoxypropoxy]phenyl 4-(*n*-decyloxy) benzoate and 4'-[(*s*)-4-methylhexyloxy]phenyl 4-(*n*-decyloxy) benzoate, respectively. Available from Displaytech, Inc., 2200 Central Avenue, Boulder, CO 80301.
  - [9] T.P. Rieker, N.A. Clark, G.S. Smith, D.S. Parmar, E.B. Sirota, and C.R. Safinya, *Phys. Rev. Lett.* **59**, 2658 (1987).
  - [10] J.-Z. Xue, N.A. Clark, and M.R. Meadows, *Appl. Phys. Lett.* **53**, 2397 (1988).
  - [11] N.A. Clark, T.P. Rieker, and J.E. Maclennan, *Ferroelectrics* **85**, 467 (1988).
  - [12] J.E. Maclennan and N.A. Clark, *Liquid Cryst.* **7**, 753 (1990).
  - [13] W.J.A.M. Hartmann (unpublished).
  - [14] P. Maltese, J. Dijion, T. Leroux, and D. Sarrsin, *Ferroelectrics* **85**, 265 (1988).
  - [15] The FLC mixture is a 1:1:2 mixture of W7, W37, and W82 with W37 being 4'-[(*s*)-2-propyloxypropyloxy]phenyl 4-(*n*-dodecyl) oxybenzoate. Also available from Displaytech, Inc.
  - [16] A.A. Chernov, *Kristallografiya* **7**, 895 (1963) [*Sov. Phys.—Crystallog.* **7**, 728 (1963)]; J.Z. Xue and N.A. Clark (unpublished).
  - [17] N.A. Clark and T.P. Rieker, *Phys. Rev. A* **37**, 1053 (1988).
  - [18] M.A. Handschy and N.A. Clark, *Ferroelectrics* **59**, 69 (1984).
  - [19] J.E. Maclennan, M.A. Handschy, and N.A. Clark, *Liquid Cryst.* **7**, 787 (1990).
  - [20] N. Hiji, Y. Ouchi, H. Takezoe, and A. Fukuda, *Jpn. J. Appl. Phys.* **27**, L1 (1988).
  - [21] A. Fukuda, Y. Ouchi, H. Arai, and H. Takezoe, *Liquid Cryst.* **6**, 1055 (1989).
  - [22] Z. Zhuang, N.A. Clark, and J.E. Maclennan, *Jpn. J. Appl. Phys.* **29**, L2239 (1990).
  - [23] Z. Zhuang, N.A. Clark, and J.E. Maclennan, *Liquid Cryst.* **10**, 409 (1991).
  - [24] J.-Z. Xue, Ph.D. dissertation, University of Colorado,

- 1989 (unpublished).
- [25] Z. Zou and N.A. Clark (unpublished).
- [26] I. Dahl and S.T. Lagerwall, *Ferroelectrics* **58**, 215 (1984).
- [27] S.A. Pikin and V.L. Indenbom, *Ferroelectrics* **20**, 151 (1978).
- [28] P.C. Willis, N.A. Clark, and C.R. Safinya, *Liquid Cryst.* **11**, 581 (1992).
- [29] R.B. Meyer, *Phys. Rev. Lett.* **22**, 918(1969).

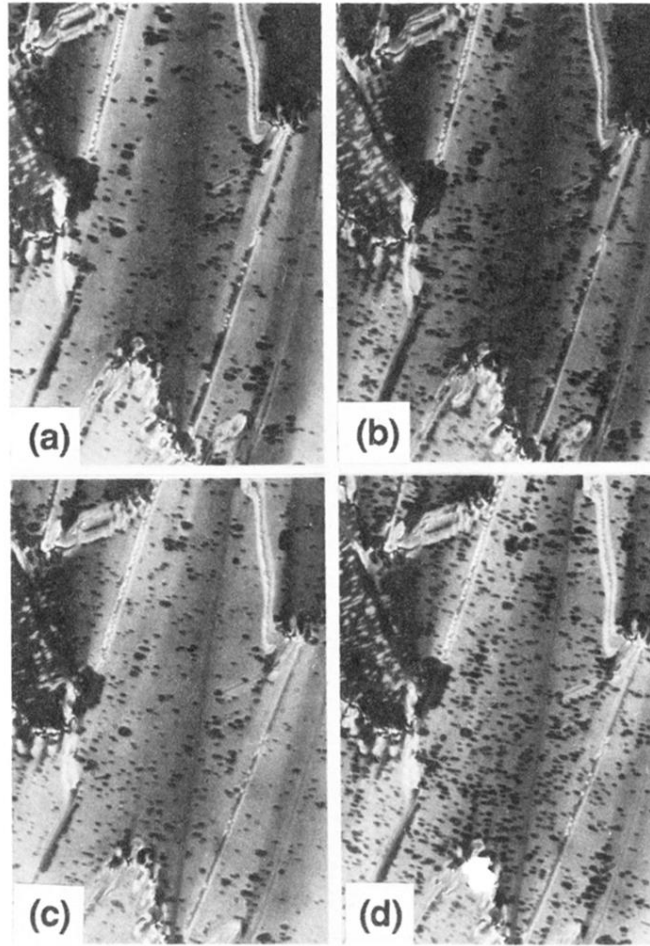


FIG. 10. Photomicrographs of the reversing domains when  $T = 25^\circ\text{C}$  and the applied field is higher.  $V = 12\text{ V}$  in (a) and (b) with  $\Delta t$  being 1.368 ms and 1.418 ms, respectively. The applied field is 15 V in (c) and (d) with the  $\Delta t$  being 0.911 ms and 0.942 ms, respectively. Notice that the domains are getting more symmetric and homogeneous nucleation dominates the switching process.

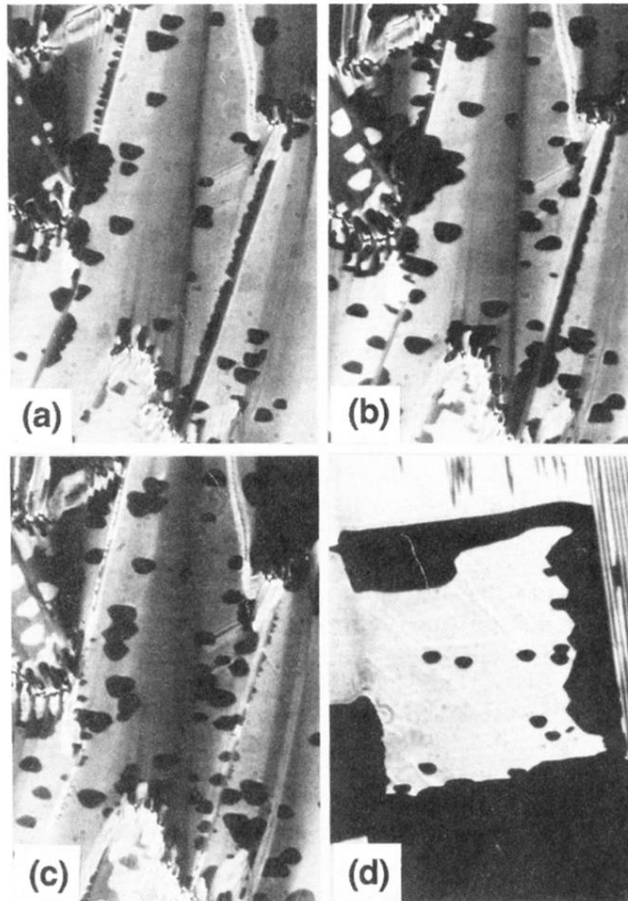


FIG. 11. Photomicrographs of the reversing domains at higher temperatures. (a)  $T = 30^\circ\text{C}$ , applied field  $V = 5$  V, and the time  $\Delta t = 3.30$  ms. (b)  $T = 35^\circ\text{C}$ ,  $V = 5$  V,  $\Delta t = 2.183$  ms. (c)  $T = 40^\circ\text{C}$ ,  $V = 3$  V,  $\Delta t = 2.764$  ms. (d). The sample is shear aligned and the material is the second FLC mix.  $T = 40^\circ\text{C}$ ,  $V = 1$  V, and  $\Delta t = 1.49$  ms. Notice that the domains getting more and more symmetric about the chevron direction.

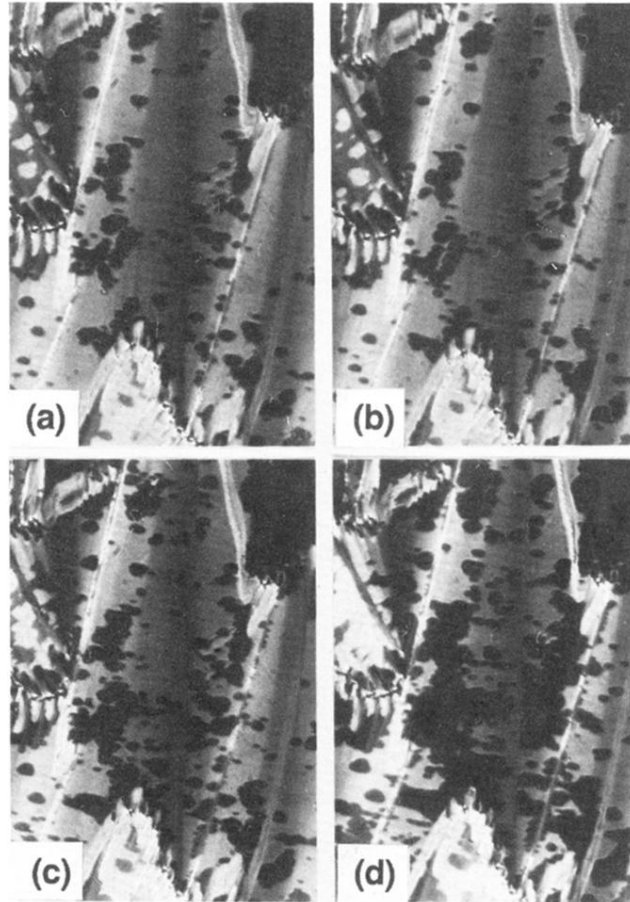


FIG. 2. Heterogeneous nucleation of reversing domains in SSFLC's. The sample temperature  $T = 35^\circ$  and the applied voltage  $V$  is 5 V. Pictures taken after the field is applied to the cell for  $\Delta t$  which is (a) 0.997 ms, (b) 1.368 ms, (c) 1.973 ms, and (d) 3.10 ms. The arrow is  $70 \mu\text{m}$  in length.

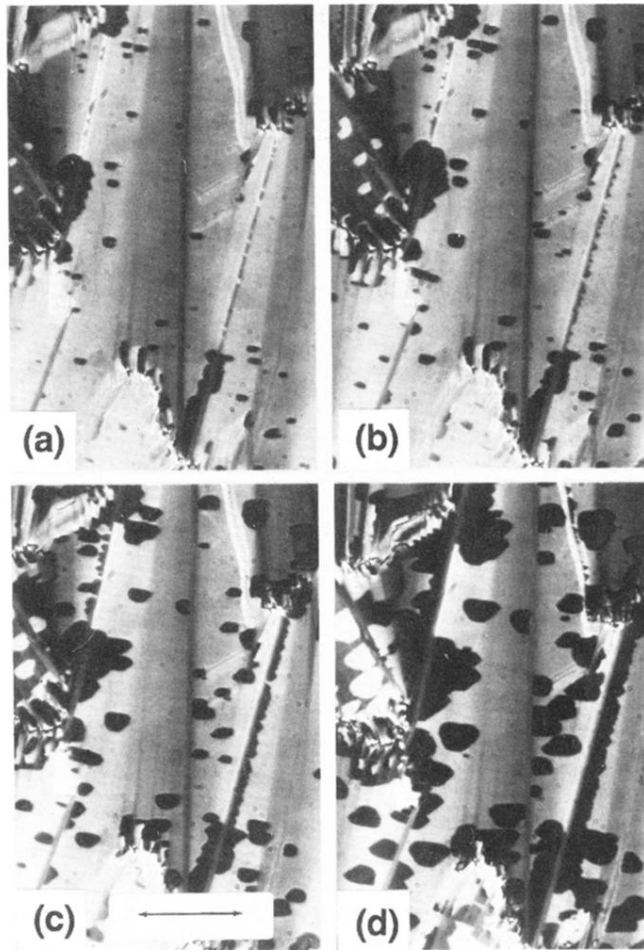


FIG. 3. Homogeneous nucleation of reversing domains in SSFLC's. The sample temperature  $T = 40^\circ\text{C}$  and the applied field  $V$  is 5 V.  $\Delta t$  is (a) 3.48 ms, (b) 3.48 ms [same as for (a)], (c) 3.64 ms, and (d) 3.86 ms.



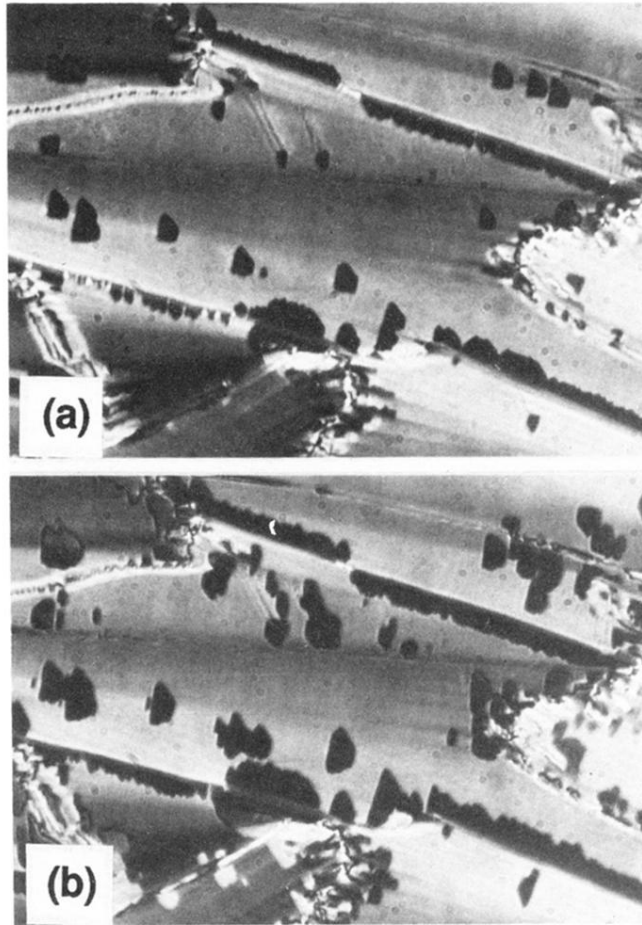


FIG. 9. Photomicrographs of the reversing domains when  $T = 25^\circ\text{C}$ . The pictures were taken when the (a) 5 V voltage is applied for 5.582 ms and (b) 8 V applied for 4.243 ms. Notice that the asymmetry of the domains is becoming less pronounced in (b).